Field Methods and Instrument Types for Using Seismic Monitoring of Bedload in Sand-Rich Gravel Bed Ephemeral Channels

J. Mitchell McLaughlin, New Mexico Tech, Socorro NM, john.mclaughlin@student.nmt.edu
Susan Bilek, New Mexico Tech, Socorro NM, susan.bilek@nmt.edu
Daniel Cadol, New Mexico Tech, daniel.cadol@nmt.edu
Jonathan B. Laronne, Ben Gurion University of the Negev, Beer Sheba, Israel, john@bgu.ac.il
David Varyu, United States Bureau of Reclamation, Denver CO, dvaryu@usbr.gov

Abstract

Environmental seismology is a relatively new field of study involving the use of seismic signals to characterize surface processes, including sediment transport and other river processes. Published studies of bedload monitoring have typically used a relatively small number of seismic instruments, often at considerable distances from active channels, to characterize signals generated by fluvial processes. We focused here on data collected along a sand-rich (~30% < 2mm) gravel ephemeral channel, where even shallow water moves high bedload fluxes during monsoon-driven flash flood events. Within the Arroyo de los Pinos watershed in central New Mexico, we have deployed several different types of seismic instrumentation, including very sensitive broadband sensors and easy-to-deploy high-frequency nodal sensors, at various distances from the channel and in different geologic conditions. These instruments are one component of the experimental watershed that also includes Reid-type continuously monitoring bedload slot samplers, suspended sediment pump samplers, pressure transducers, and rain gauges to capture the hydrologic, meteorologic, and sedimentologic conditions during flow events. Because flow events frequently include multiple concurrent fluvial processes, and seismic sensors are subject to a wide variety of environmental noise sources, it is essential to understand how the field deployment, site selection, and instrument type affect seismic data and interfere with target signals. Here we describe our seismic field methods, including site selection, instrument deployment strategies, and characterization of anthropogenic background noise. We also examine seismic data from a mid-sized flood recorded on multiple instruments to determine how instrument type and deployment conditions affect recorded signals. Seismic stations located 21 m from an active channel recorded seismic signals associated with bedload transport even at very shallow flow depths, but closer stations are better able to resolve high frequency signals. Anthropogenic noise has some influence on the range of signals associated with bedload transport, but as distance from anthropogenic sources increases, the frequency of these signals decreases below that of target signals. Rainfall has a significant effect in the range of bedload-associated signals, although these signals vary considerably between instruments, likely depending on their specific deployment location.

Introduction

Fluvial bedload transport remains a challenging, costly, and frequently hazardous process to monitor. Physical sampling is generally limited to rivers with permanent bedload sampling infrastructure, and many surrogate instruments still require permanent installations. Bedload monitoring instruments include slot samplers designed to capture bedload as it passes near the opening of a large pit (Laronne et al., 2003), geophones designed to record impacts of large transported particles (Turowski et al., 2011), and pipe microphones designed to record acoustic signals following particle impacts (Mizuyama et al., 2010). Use of these instruments include challenges: limitations on the volume of collected sediment (Stark

et al., 2021), sensitivity to particular grain sizes (Roth et al., 2016), and covering-effects due to the settling location of some sediment (Stark et al., 2019).

Bedload monitoring in ephemeral channels is particularly challenging. Due to the flashy and unpredictable nature of storms generating flows in these systems, all monitoring techniques must be functional without an operator present. For example, in the desert southwest of the United States, many ephemeral channel flow events are driven by short duration, localized, and torrential rainfall characteristic of the North American monsoon. Because flow events in arid and semiarid regions are known to transport large amounts of sediment as bedload (Laronne and Reid, 1993), and ephemeral streams make up the vast majority of streams in the southwestern U.S. (Levick et al., 2008), bedload transport is a major component of the overall sediment budget of this region.

In recent years, seismic instruments have emerged as a potential surrogate tool with which to study bedload transport (e.g., Burtin et al., 2008; Schmandt et al., 2013). As bedload particles impact the bed, they generate elastic waves along the surface that can be recorded on seismometers as vibrations. These vibrations propagate through the shallow subsurface to seismic instruments placed safely away from active channel processes. Additionally, because seismic instruments are designed to collect data during long periods of time, there are no limitations on the total mass of detected bedload. Thus, the ability to accurately detect and quantify bedload flux with seismic equipment can reduce the costs, maintenance, and hazards associated with traditional bedload monitoring equipment.

A disadvantage of the seismic recording of bedload transport is the myriad of other captured seismic signals. Seismometers register ground vibrations from a wide variety of sources. These may include short-duration sources like earthquakes and explosions, but also omnipresent global background noise due to ocean waves (Ardhuin et al., 2015; Bromirski et al., 2005). Most of these sources can be identified and filtered from the seismic time series. More relevant to seismic studies of fluvial processes are local sources of noise. Rainfall is an important source of seismic noise during flood events, and the resultant noise signal varies depending on drop size and characteristics of the seismic deployment (Bakker et al., 2022; Dean, 2018). Wind can also generate ground vibrations (Withers et al., 1993). Both rain and wind are subject to effects from vegetation. Vegetation coverage surrounding seismic instruments is expected to have a homogenizing effect on raindrop size (Roth et al., 2016), while amplifying the effects of wind (Johnson et al., 2018). Wind and rain frequently occur concurrently with bedload transport events.

The most common technique for resolving vibrations generated by a specific surface process such as bedload transport is to isolate the frequencies that are associated with the process of interest. Early seismic studies of fluvial processes noted hysteresis of seismic signals with respect to water depth over the course of a Himalayan monsoon season, which Burtin et al. (2008) attributed to temporal changes in sediment supply. They interpreted this pattern to suggest the seismic data were largely influenced by bedload transport (Burtin et al., 2008). Further research noted that during one controlled flood experiment, hysteresis was only observed in high frequency signals (15-45 Hz), while lower frequency signals (0.5-2 Hz) scaled solely with water depth (Schmandt et al., 2013). These studies suggest links between high frequency signals and bedload transport, as well as low frequency signals and water discharge. Other experimental and modeling studies support these links (Schmandt et al., 2017; Tsai et al., 2012; Gimbert et al., 2014).

Seismic techniques show strong promise for studying fluvial processes. However - as with every type of signal - the ability to constrain fluvial processes with seismic data requires attention to instrument deployment strategies and noise characterization. Instrument type, channel-station distance, and the general study location will all affect the seismic data generated during flow events. Here we present seismic data from a unique experimental

watershed, the Arroyo de los Pinos (ADLP), to explore issues of instrument type, channel distance, and relevant noise recordings. Because we have a range of instruments to capture flow and noise signals, this location is ideal for testing the effect of these parameters on the fluvial-related seismic signals.

Arroyo de los Pinos Experimental Watershed

An extensive network of seismic and hydrologic equipment within the ADLP experimental watershed was used for this study. The Arroyo de los Pinos is an ephemeral tributary to the Mid-Rio Grande in central New Mexico (Figure 1), characterized by monsoon-driven storms primarily occurring in the months of July and August. Although the Arroyo de los Pinos, like many ephemeral channels in arid environments, transports large quantities of sediment during flood events (Stark et al., 2021), it typically flows less than 36 hours per year. Because the vast majority of streams in the American southwest are ephemeral (Levick et al., 2008), this watershed is used to gain understanding of the rapid and unpredictable flow events that comprise the region during the North American monsoon. Additionally, the watershed is used to develop efficient and safe techniques with which to study these events.

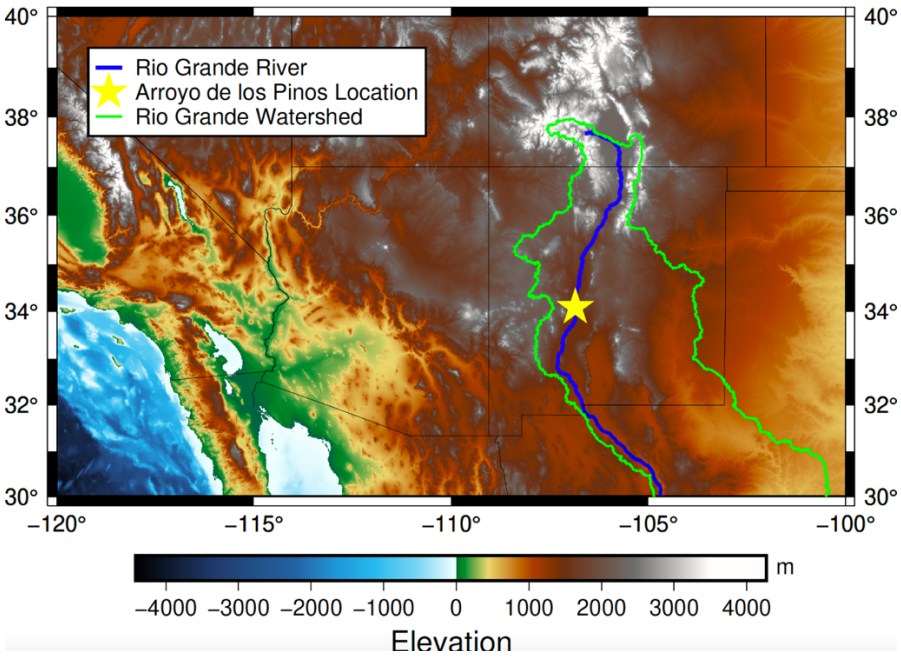

Figure 1: Location of Arroyo de los Pinos (ADLP) within the Rio Grande watershed (outlined green) in New Mexico, southwestern United States.

The ALDP watershed (area 32 km^2) consists of 71 seismic instruments, ~12 pressure transducers, 4 rain gauges, and a state-of-the-art sediment monitoring station at the channel outlet. Pressure transducers sample at 2 minute intervals, while rain gauges sample at 1 - 15 minute intervals depending on the location. Due to geomorphic changes throughout the course of the monsoon season, pressure transducers upstream of the outlet provide only a rough estimate of water depth. At the outlet of the channel, the concrete sediment-monitoring installation allows a precise estimate of water depth.

The seismic network is distributed across four reaches of the ADLP and contains 66 three-component high frequency seismometers (referred to as “nodes”) and 5 broadband seismometers (Figures 2 and 3). Broadband seismometers are capable of resolving a wide range of frequencies, including the very low frequency band that is globally observed and dominated by ocean processes (e.g., Ardhuin et al., 2015). The node seismometers are well suited to capture higher frequency signals (>5 Hz), sufficient for the purpose of this research.

The nodes and one broadband seismometer sample at 1000 samples/second, and the remaining four broadbands sample at 500 samples/sec. This high sample rate is necessary to resolve the high frequency signals attributed to bedload transport.

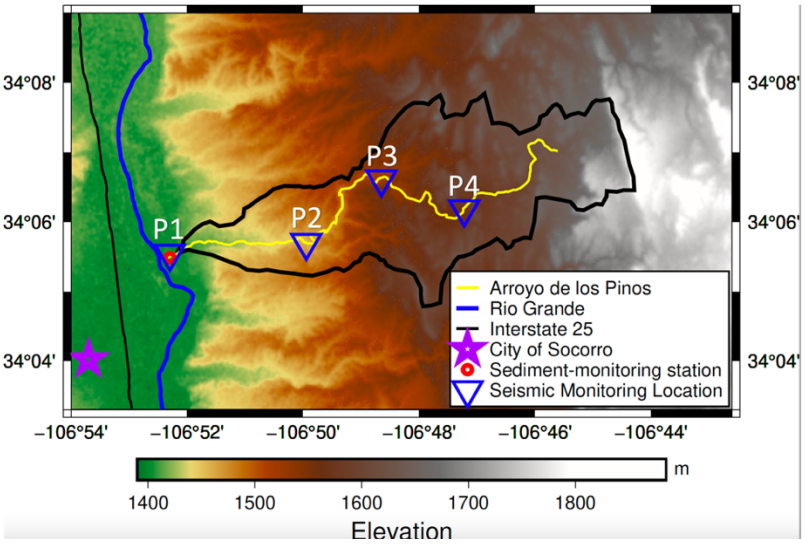

Figure 2: ADLP seismic monitoring locations.

Figure 3: Installation of a seismic node (left) and two types of broadband seismometers deployed adjacent to the ADLP. Broadband sensors are buried underground, with surface vaults (red circle) housing the data loggers and other electronics.

Methods

Seismic Data Analysis

Seismic data are acquired as a time series with units specific to the instrument being used. Using manufacturer-defined instrument response, raw seismic data are converted to ground velocities. Seismograms included here (example Figure 4a) provide a time series of this ground motion recorded at a sensor. Traditionally, seismograms are frequently used to identify arrivals of specific seismic phases in earthquake studies, however fluvial studies often transform the data into the frequency domain and explore the temporal evolution of seismic energy at different frequencies using spectrograms (Figure 4b).

For our analysis, we divided the ground velocity time-series into a series of small, overlapping windows with length of 2^{11} samples and a 50% overlap. For each window, we applied a Fast-Fourier Transform algorithm (Cooley and Tukey, 1965) to obtain the power-spectral density (PSD)—the power, per Hz, at all frequencies up to the Nyquist, or one half of

the sampling interval. To allow for the easiest comparison of seismic power between two locations, we present these power-spectral densities. To compute these for a time window of interest, we again used smaller, overlapping time-series for which we compute the PSD. We then averaged these PSDs to obtain an overall value (Welch, 1967). When comparing noise levels between two locations (see tables 2 and 3), we calculated the median power-spectral density within a desired range of frequencies using the overall PSD.

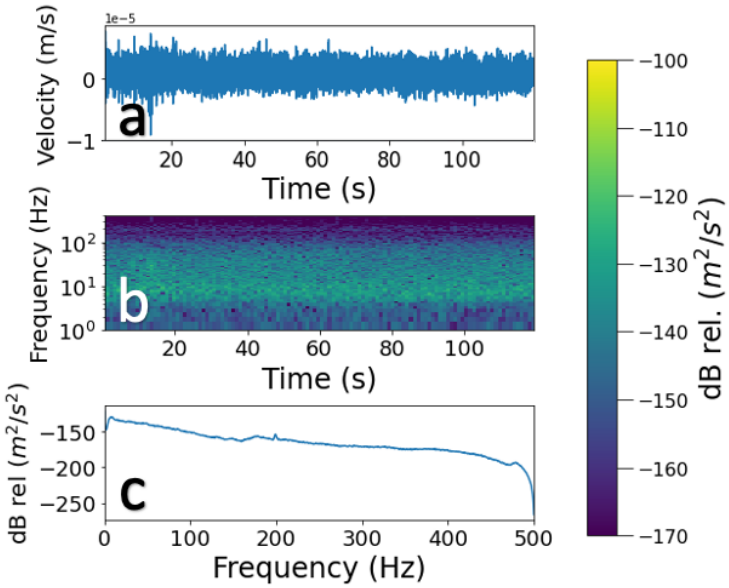

Figure 4: a) Sample ground velocity seismogram for a two-minute period used to compute spectrogram and power-spectral density shown in panels b and c. b) Spectrogram. c) Power-spectral density.

Effect of Channel-Station Distance on Target Signals

We analyzed a single flow event within the ADLP watershed to characterize seismic signals at two locations and on several instruments. To determine how the distance between seismic instruments and the active channel affects seismic signals, we examined data from two pairs of nodes - one pair at the outlet of the channel, near P1, and one pair at the first upstream location, P2 (Figure 5). Two nodes at the outlet were deliberately deployed at different distances from one another to examine the effects of attenuation. The pair of nodes at the upstream location are adjacent, but vary in distance from the channel such that one node would avoid a low-lying bar that can become activated in a very large flood. We computed seismic power spectral density (PSD) to obtain seismic power at each frequency for the full flow event and present these as spectrograms. These allow easier visualization of temporal variations in seismic power with frequency (see previous section).

We selected a two minute period during which flow is confirmed by pressure transducers and compare those PSDs with a period of time during which no flow occurred. For all PSD calculations, times without apparent rainfall noise were selected. A lack of broadband noise (elevated seismic amplitudes across all measured frequencies) was used to assume no rainfall was present, as determined elsewhere (Roth et al., 2016, Bakker et al., 2022, Dietze et al., 2019) and tested locally at the ADLP.

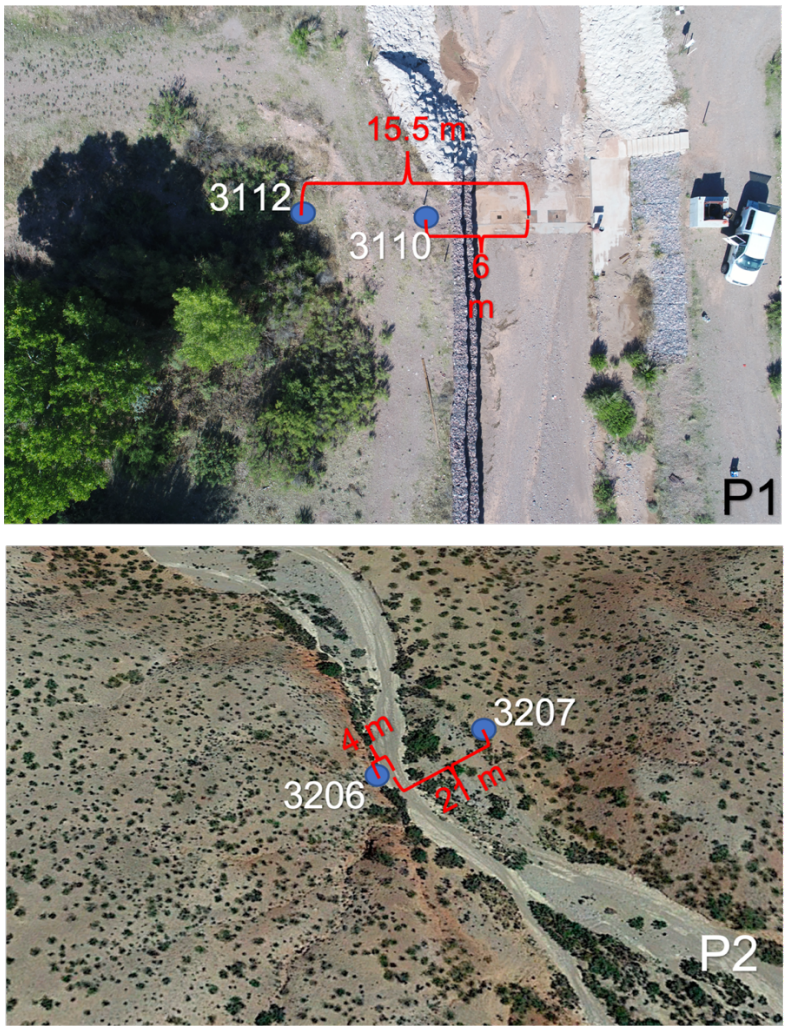

Figure 5: Location of seismic node station pairs used for this study at P1 and P2 locations. Nodes are labeled according to their station names (white numbers 3XXX). Distance (red) labels indicate spacing from channel center to node location as determined within Google Earth.

Effect of Anthropogenic Noise on Target Signals

Seismic studies of fluvial processes require adequate signal to noise ratio: seismic noise generated by a flow event must be distinguishable from background noise. To determine the prominence of anthropogenic noise within a target frequency range, we examined seismic amplitudes at frequencies between 30 and 80 Hz—a frequency band characteristic of fluvial processes and well within the range expected to be dominated by bedload transport (Schmandt et al., 2017). Amplitudes in this frequency range were examined across the four seismic-monitoring locations, which exist at increasing distances from a major interstate highway (I-25) and the city of Socorro (Figure 2; Table 1). Because these seismic noise signals likely vary according to time-of-day, roughly tracking human activity patterns (Diaz et al., 2017), we examined seismic PSD levels over the same time period.

We also examined the seismic noise signature generated by a passing train. These signals, which appear as 3-5 minute increases in seismic power primarily in low frequencies, have been characterized using observations of passing trains, followed by examination of seismic data. Their observed frequency content is also in line with expectations based on previous research (Quiros et al., 2017). At the ADLP P1 location, the peak frequency of these signals lies between 2 and 8 Hz, although elevated power above 30 Hz is observed in spectrograms, suggesting that signals from passing trains may overlap with signals analyzed for the purpose

of bedload monitoring. To determine the extent to which train-generated signals interfere with the frequencies associated with bedload transport at different distances, spectrograms and power-spectral densities were computed for a time period known to contain a passing train (distance in Table 1) occurring at all seismic stations.

Location	Distance from I-25 (km)	Distance from Socorro (km)	Distance from Train Tracks (km)
P1 Main Site	2.1	3.9	1.6
P2 Upstream Site	6.1	6.8	5.1
P3 Upstream Site	8.2	9.4	7.4
P4 Upstream Site	10.3	11.1	9.4

Table 1: Closest distance between anthropogenic sources and ADLP seismic monitoring regions shown in Figure 2. Distances were measured on Google Earth.

Effect of Rainfall Noise on Target Signals

Rainfall generates seismic signals when drops splatter onto the surface above and near seismic instruments (Bakker et al., 2022). Because rainfall generates noise at a wide range of frequencies (Roth et al., 2016; Dietze et al.; 2019), it represents a significant source of noise that may overlap with bedload signals. Because various factors affect the noise generated by rainfall, including the depth of the sensor and surrounding vegetation (Dean et al., 2018; Roth et al., 2016), we examined seismic signals during recorded periods of rainfall at different monitoring locations and on different instrument types.

To analyze these effects, we used spectrograms to identify a short period of time during which heavy rainfall, but no in-channel flow occurred at the P1 monitoring site. To confirm the presence of rainfall during this time, we compare seismic spectrograms with NEXRAD radar imagery (NOAA NWS, last accessed October 7, 2022). We downloaded six hours of radar imagery with unique images provided every 2-3 minutes and save the time and color value from each frame at the ADLP P1 site. The color value is saved as an RGBA value - a set of four values that describe the red, green and blue color components as well as a value that describes opacity. This analysis is performed to ensure that broadband noise is associated with rainfall. To estimate rainfall intensity, we use a tipping bucket rain gauge present at the site, recording the rainfall depth every 15 minutes according to a number of new bucket tips, equivalent to 0.01 inches of rainfall. Although this rain gauge appears to have a significant timing error and could not be used to correlate rainfall with broadband noise, maximum rainfall intensity could be estimated. Having identified rainfall in the seismic record, we compared the PSD of these seismic signals generated by rainfall for various instruments.

Results

Source-Station Distance

Spectrograms and PSDs produced for the pair of nodes at the P2 upstream site indicate clear differences in frequency and amplitude content with varying distance to the channel center (Figure 6). The nearest node at 4 m from the channel center recorded greater power-spectral density (in dB relative to m^2/s^2, per Hz) across the frequency domain than the node 21 m from channel center. The PSD from the nearer node has a -133 dB maximum at a peak frequency of 62 Hz, while the more distant node has a maximum PSD of -149 dB at a peak frequency of 41 Hz (Figure 6b) Additionally, signals at higher frequencies (100-150 Hz) show

similar decreases in PSD with increased distance from the channel; At 150 Hz, the nearer node has a PSD of -141 dB, much more than the more distant node at -171 dB.

The two nodes at P1 show a similar trend, with higher PSD at higher frequencies at the node closest to the channel. The nearer node has peak PSD of -120 dB at a peak frequency of 51 Hz, while the more distant node has peak PSD of -128 dB at a peak frequency of 7 Hz. Even with relatively shallow flows (~10 cm max flow depth at P2 and 18cm max flow depth at P1), signals related to flow events have PSD values well above background noise at both near and far nodes, although the measurement frequency is important. At nodes further distanced from the channel, high-frequency (>100 Hz) signals have PSDs approaching those of background noise. High frequency signals are observable above background noise even when water depth is merely 6 cm and at 21 m from the active channel (Figure 6a, P2).

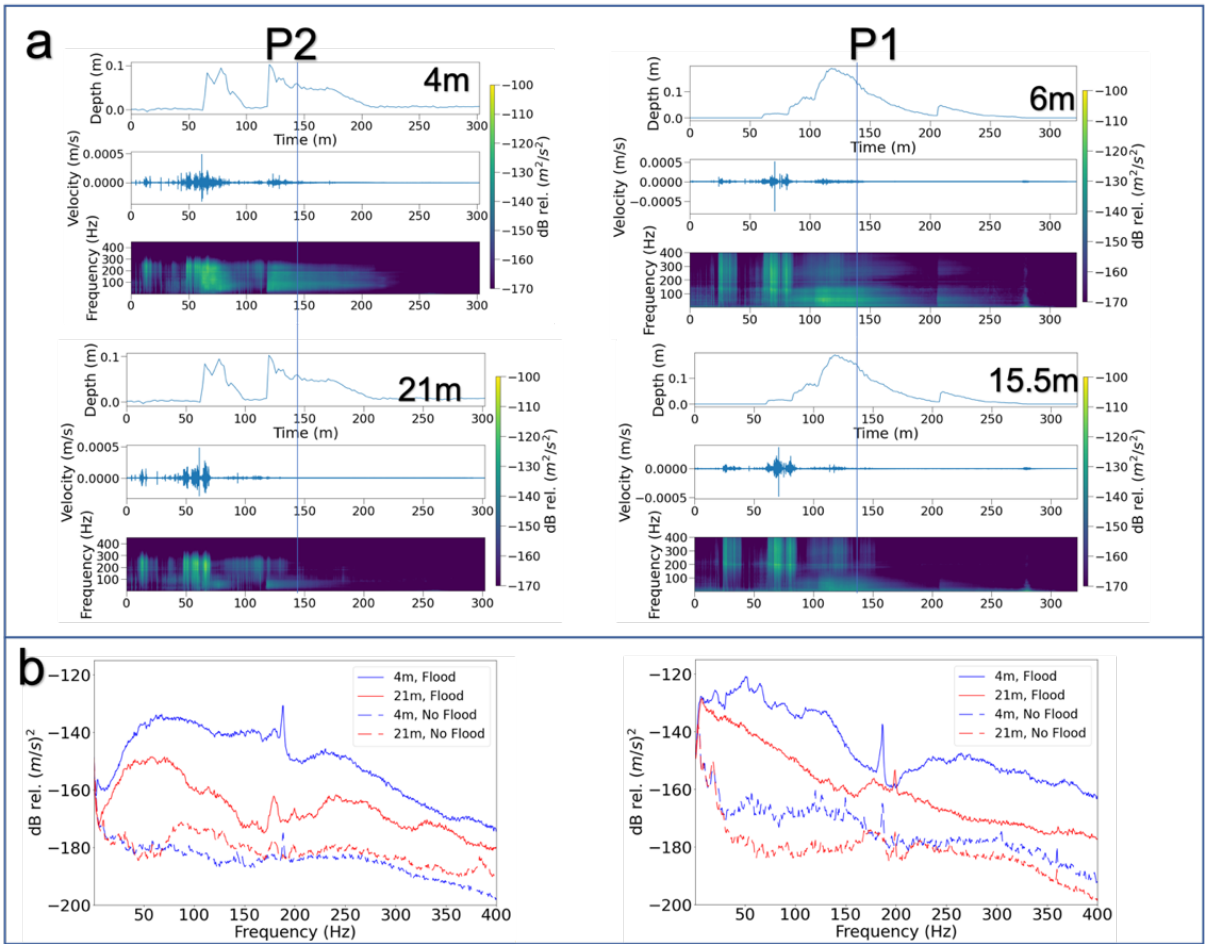

Figure 6: (a) Spectrograms from near and far stations for pairs of nodes at site P2 and P1. Blue lines indicate times used for power-spectral density calculation during flows. (b) Power-spectral density for each station; time periods were selected during flow (solid) and without flow (dashed).PSDs during flow were computed for a two minute period beginning at 2021-08-23 11:22 (UTC) at P2 and 2021-08-23 10:54 UTC. Quiet periods were two minute periods beginning on 2021-08-23 00:30 for both stations.

Node	Location	Distance from channel (m)	Approximate Water Depth (cm)	Median PSD (30-80 Hz) (dB)	Median PSD (100-150 Hz) (dB)	Median PSD—no flow (30-80 Hz) (dB)
3206	P2	4	7	-136	-140	-181
3207	P2	21	7	-150	-162	-180
3110	P1	6	13	-128	-134	-160
3112	P1	15.5	13	-140	-156	-172

Table 2: Median power values within two frequency ranges while flow occurred (see Figure 6).

Anthropogenic Background Noise

Background noise signals are the highest at site P1 which is closest to anthropogenic sources such as the highway and the city (Table 1). The peak frequency for this anthropogenic noise is low (<50 Hz), but this leads to small increases in PSD values in the 30-80 Hz frequency range associated with bedload transport (Figure 7). Some noise can be seen in spectrograms at > 20 Hz frequencies towards the end of the time window, possibly due to wind-vegetation effects.

Background noise PSDs are approximately -169 dB within the range of frequencies associated with bedload transport (30-80 Hz) at P1MS, nearest anthropogenic sources, while slightly lower (-172 to -177 dB) at upstream locations (Table 3). These background noise PSDs are ~20 dB lower than noise levels generated by a 13 cm flow at the outlet of the channel (see Figure 6). This suggests that while anthropogenic background noise can be observed at each of the monitoring locations, target flow signals, even at very shallow water depths, generate sufficiently high frequencies with higher power than the background noise.

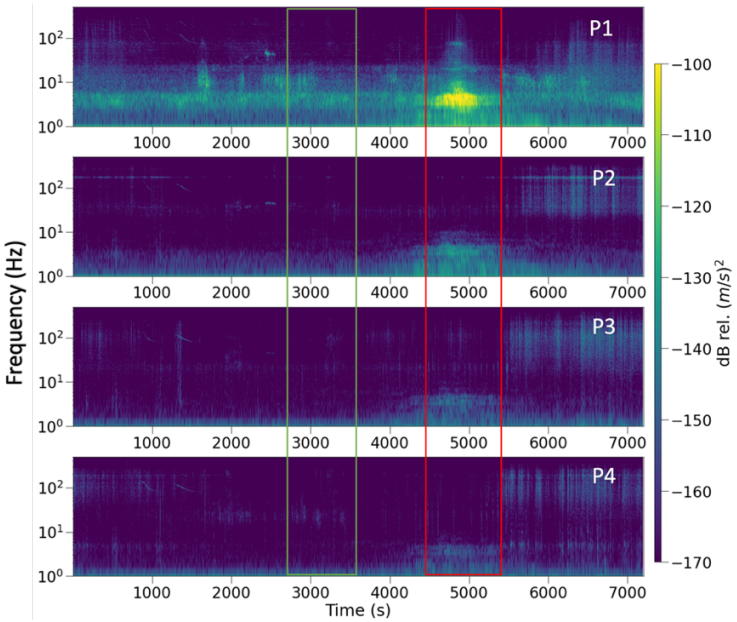

Figure 7: Seismic spectrograms for a 2 hour window beginning 2021, August 23 00:00 UTC. Spectrograms are computed from the downstream-most seismic node at each location (station names 3100, 3200, 3300, 3400; See Figure 2 for site locations). PSD computations for background noise and train signals were performed over the time intervals highlighted in green (see Fig. 7) and red respectively.

Train Signals

Trains passing within 1.6 km from the P1 site generate high levels of noise, as observed in the relevant PSDs. These signals are primarily at low frequencies, although elevated signals are also observed within the 30-80 Hz range (Figure 7). Upstream sites also show elevated PSD levels as a result of the passing train at frequencies below 10 Hz, but above 30 Hz there is no indication of an influence from the train at these sites; PSD values remain orders of magnitude lower than those generated by small-medium flow events (Table 3).

Location	Median Background Noise Power (30-80 Hz) (dB)	Median Train PSD (30-80 Hz) (dB)	Median flow PSD (30-80 Hz) (dB)
P1 Main Site	-168.6	-156.7	-126 dB
P2 Upstream Site	-176.2	-172.6	
P3 Upstream Site	-173.2	-169.9	
P4 Upstream Site	-172.3	-170.1	

Table 3: Median PSD within the specified time-windows (see Figure 7) and frequency range for background noise and a passing train. A reference median PSD taken from the flow at P1 (described in section 4.1) is shown in column 4. Stations used at four sites are 3100, 3200, 3300, 3400.

Rainfall Noise

Radar data representing the monitoring site are correlated with broadband seismic noise, with increased seismic power within the full 1-500 Hz frequency range well explained by rainfall during periods of heavy rain. The radar imagery data provide color values (red, yellow, green, and beige) to indicate high, moderate, low, and nonexistent rainfall intensity respectively. These colors are consistent with the levels of broadband seismic noise visible in spectrograms. Locally collected rain gauge data shows a high rainfall intensity at approximately the same time, but with a timing error of approximately 15 minutes relative to the radar data. We use the rain gauge only to get an estimate of maximum average rainfall intensity of 0.37 mm/min (over the course of a 15 minute sampling interval), disregarding the timing. Average intensities as low as 0.034 mm/min can be identified in the seismic signal.

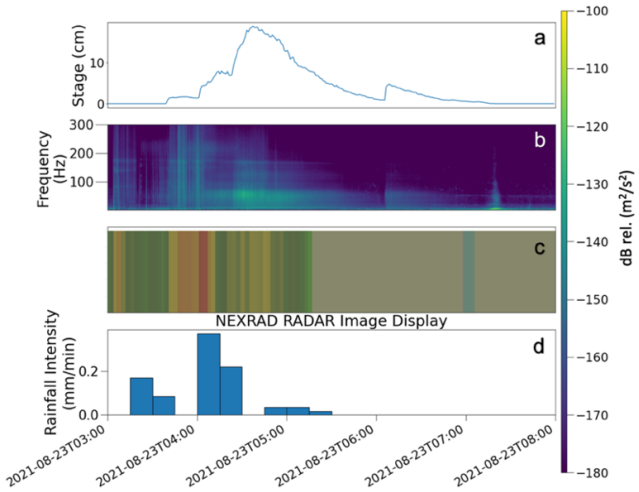

Figure 8: a) August 23, 2021 stage hydrograph. b) Seismic spectrogram computed from a seismic node (station name 3110) depicting the temporal evolution of the frequency and amplitude content taken from a five hour time window including the event. Times labeled are local times (MDT). c) NEXRAD Radar Image colors, with heavy, moderate, and light rain being indicated by red, yellow, and green respectively, surrounding the location of the P1 seismic station. d) Rainfall intensity at the P1MS station.

Discussion

Optimal deployment of seismic instruments alongside ephemeral channels for the purpose of bedload transport monitoring is dependent on the ability to record target signals above anthropogenic and rainfall-generated noise. Since anthropogenic noise, like any seismic signal, attenuates such that high-frequency noise is rapidly removed with increasing distance from the source, the effect of this noise depends on the distance of the instrument from the studied channel, the distance of the instrument from anthropogenic sources, and the frequency range being used to study bedload transport. As rainfall generates noise at every observable frequency, minimization of rainfall effects depends solely on the ability to limit recording of signals caused by raindrop impacts.

Optimum Channel-Station Distance

Flow events can be detected for very small flows (<6 cm depth) from distances up to 21 m (Figure 6) but as suggested by previous efforts for seismic monitoring of bedload transport, the ability to capture high frequency signals is important. Previous studies suggest correlation between seismic signals in the 15-45 Hz range (Schmandt et al., 2013), the 20-100 Hz range (Schmandt et al., 2017), and the 30-50 Hz range (Bakker et al., 2020) with bedload flux. Our previous work also suggests that influence of turbulence-generated flow signals occurs at lower frequencies, in agreement with modeled results (Tsai et al., 2012; Gimbert et al., 2014). Another important consideration for the determination of distance and frequency range to capture bedload transport is the expected particle size of transported bedload: finer-grained particles generating higher frequency signals (Huang et al., 2007). Thus, attempts to monitor the transport of fine-grained bedload particles should include seismic stations in close proximity to the channel due to the high frequency attenuation. At the Arroyo de los Pinos sediment-monitoring station, where the average size of bed-surface particles within the thalweg of the channel is 5 mm (Stark et al., 2021), a distance of 15 m suffices to resolve high-frequency noise during small-medium flow events. For shallower flows, transporting ever finer-grained bedload, a reduced channel-station distance may be necessary.

Anthropogenic Noise Considerations

Anthropogenic noise is clearly visible at the P1MS site, but the anthropogenic noise levels within the 30-80 Hz frequency range we associate with bedload transport at the site is well below noise levels generated during flow events. When studying channels with more prominent anthropogenic sources than those near the Arroyo de los Pinos, examining background noise levels will be required to determine the extent to which they may obscure target signals.

Because smaller diameter particles are expected to generate relatively high frequencies as they impact the ground (Huang et al., 2007), fine-grained channels may still be monitored for bedload-transport with seismic instruments even in relatively close proximity to anthropogenic sources, as fine-grained particles may generate signals that extend to higher frequencies than anthropogenic sources. Because these signals attenuate quickly, however, fine-grained channels should be equipped with seismic stations as close to the active channel as possible. Physical models have demonstrated that seismic noise from bedload transport is dominated by the largest particles (Tsai et al., 2012). Thus, since seismic amplitudes generated by the movement of small particles are expected to be small, seismic stations deployed too far from fine-grained channels may not be capable of registering bedload transport signals at all.

Minimizing the Effect of Rainfall in Seismic Deployments

Since rainfall generates noise across all frequencies, it will contribute seismic signals in the range of frequencies associated with bedload transport. Because there is often a time delay between the time of rainfall and the beginning of fluvial processes (Glasgo, 2022), rainfall does not always pose a problem for bedload transport studies. In cases where bedload transport occurs simultaneously with rainfall, however, rainfall-generated noise should be minimized.

Deployment depth is a large control on rainfall-generated noise (Dean et al., 2018). Relatively permanent instruments, including the broadbands within the Arroyo de los Pinos watershed, have sensors deployed more than 50 cm below the surface with surface installed electronics and GPS clocks for timing. Seismic nodes are deployed less than 7 cm below the surface for onboard GPS timing to connect to satellites. While researchers should aim to deploy seismic nodes as deep as GPS limitations allow, these depths will be limited. Other considerations, such as site geology and vegetation, will also affect the rainfall signals. Previous research along an alpine river found high frequency rainfall-related signals observed only near a large boulder (Burtin et al., 2016). This suggests that deployments within differing lithologies may also be present with distinct rainfall-related signals. Vegetation canopy may reduce both the raindrop size and impact velocity (Roth et al., 2016), although vegetation can also impact wind-generated noise imparted into the subsurface. The best deployment strategy may be a mixed-mode seismic array with one deeply buried sensor away from vegetation, in conjunction with additional easier to deploy nodes, all placed as close to the channel as possible.

Conclusions

With the following understandings in place, seismic studies can focus on building relationships between seismic signals and fluvial processes. A variety of considerations are necessary to conduct a seismic survey of bedload transport in an ephemeral channel. Although anthropogenic noise can be reduced by selecting a remote study site and examining high frequency signals, a minimal channel-station distance should be chosen to increase the signal-to-noise ratio and enhance the signal generated by the target process. High amplitude,

short duration noise events, such as passing vehicles, should be identified where possible and eliminated from analyzed seismic data.

Due to its broadband nature, rainfall presents a significant challenge to seismic studies of fluvial processes. Although rainfall noise can be minimized with deeply deployed instruments, this is not always practical for non-invasive studies as self-contained seismic nodes are considerably easier to deploy and replace. Burying seismic instruments as deep as instrument specifications allow and avoiding objects that may amplify raindrop impacts are the primary considerations with respect to minimizing rainfall noise. Mechanical devices to soften impacts or numerical methods to remove rainfall noise would be beneficial. With adequate deployment strategies and methods to correct for noise sources, seismic instruments may be a powerful tool for sustained monitoring of bedload transport in ephemeral channels.

References

Ardhuin, F., Gualtieri, L., & Stutzmann, E. (2015). How ocean waves rock the Earth: Two mechanisms explain microseisms with periods 3 to 300 S. *Geophysical Research Letters*, *42*(3), 765–772. https://doi.org/10.1002/2014gl062782

Bakker, M., Gimbert, F., Geay, T., Misset, C., Zanker, S., & Recking, A. (2020). Field application and validation of a seismic bedload transport model. *Journal of Geophysical Research: Earth Surface*, *125*(5), e2019JF005416.

Bakker, M., Legout, C., Gimbert, F., Nord, G., Boudevillain, B., & Freche, G. (2022). Seismic modelling and observations of rainfall. In *Journal of Hydrology (Vol. 610, p. 127812)*. Elsevier BV. https://doi.org/10.1016/j.jhydrol.2022.127812

Bromirski, P. D., Duennebier, F. K., & Stephen, R. A. (2005). Mid-ocean microseisms. In *Geochemistry, Geophysics, Geosystems (Vol. 6, Issue 4, p. n/a-n/a)*. American Geophysical Union (AGU). https://doi.org/10.1029/2004gc000768

Burtin, A., Bollinger, L., Vergne, J., Cattin, R., & Nábělek, J. L. (2008). Spectral analysis of seismic noise induced by rivers: A new tool to monitor spatiotemporal changes in stream hydrodynamics. *Journal of Geophysical Research*, *113*(B5). https://doi.org/10.1029/2007jb005034

Burtin, A., Hovius, N., & Turowski, J. M. (2016). Seismic monitoring of torrential and fluvial processes. In Earth Surface Dynamics (Vol. 4, Issue 2, pp. 285–307). Copernicus GmbH. https://doi.org/10.5194/esurf-4-285-2016

Cooley, J. W., & Tukey, J. W. (1965). An algorithm for the machine calculation of complex Fourier series. *Mathematics of computation*, *19*(90), 297-301

Díaz, J., Ruiz, M., Sánchez-Pastor, P. S., & Romero, P. (2017). Urban seismology: On the origin of earth vibrations within a city. *Scientific reports*, *7*(1), 1-11.

Dietze, M., Gimbert, F., Turowski, J., Stark, K. A., Cadol, D., & Laronne, J. B. (2019). The seismic view on sediment laden ephemeral flows–modelling of ground motion data for fluid and bedload dynamics in the Arroyo de los Piños. In *Sedhyd Conference 2019*.

Dean, T. (2018). The seismic signature of rain. In *ASEG Extended Abstracts* (Vol. 2018, Issue 1, pp. 1–8). Informa UK Limited. https://doi.org/10.1071/aseg2018abp068

Gimbert, F., Tsai, V. C., & Lamb, M. P. (2014). A physical model for seismic noise generation by turbulent flow in rivers. *Journal of Geophysical Research: Earth Surface*, *119*(10), 2209-2238.

Glasgo, S. (2022). Connectivity and Rainfall-Runoff Relationships in Flashy Ephemeral Systems [Unpublished masters thesis]. New Mexico Institute of Mining and Technology.

Huang, C. J., Yin, H. Y., Chen, C. Y., Yeh, C. H., & Wang, C. L. (2007). Ground vibrations produced by rock motions and debris flows. *Journal of Geophysical Research: Earth Surface*, *112*(F2).

Hunter, J. D. "Matplotlib: A 2D Graphics Environment", Computing in Science & Engineering, vol. 9, no. 3, pp. 90-95, 2007

Johnson, C. W., Meng, H., Vernon, F., & Ben-Zion, Y. (2019). Characteristics of ground motion generated by wind interaction with trees, structures, and other surface obstacles. *Journal of Geophysical Research: Solid Earth*, *124*(8), 8519-8539.

Laronne, J. B., Alexandrov, Y., Bergman, N., Cohen, H., Garcia, C., Habersack, H., Powell, D. M., & Reid, I. (2003). The continuous monitoring of bed load flux in various fluvial environments. *Erosion and Sediment Management in Rivers: Technological and Methodological Advances*, 134–145.

Laronne, J. B., & Reid, l. (1993). Very high rates of bedload sediment transport by ephemeral desert rivers. In *Nature* (Vol. 366, Issue 6451, pp. 148–150). Springer Science and Business Media LLC. https://doi.org/10.1038/366148a0

Levick, L., J. Fonseca, D. Goodrich, M. Hernandez, D. Semmens, J. Stromberg, R. Leidy, M. Scianni, D. P. Guertin, M. Tluczek, and W. Kepner. 2008. The Ecological and Hydrological Significance of Ephemeral and Intermittent Streams in the Arid and Semi-arid American Southwest. U.S. Environmental Protection Agency and

USDA/ARS Southwest Watershed Research Center, EPA/600/R-08/134, ARS/233046, 116 pp

Mizuyama, T., Oda, A., Laronne, J. B., Nonaka, M., & Matsuoka, M. (2010). Laboratory tests of a Japanese pipe geophone for continuous acoustic monitoring of coarse bedload. *US Geological Survey Scientific Investigations Report*, *5091*, 319-335

NOAA National Weather Service (NWS) Radar Operations Center (1991): NOAA Next Generation Radar (NEXRAD) Level 2 Base Data. [2021-08-23T0800-2021-08-23T1600]. NOAA National Centers for Environmental Information. doi:10.7289/V5W9574V

Quiros, D. A., Brown, L. D., & Kim, D. (2016). Seismic interferometry of railroad induced ground motions: body and surface wave imaging. In *Geophysical Journal International* (Vol. 205, Issue 1, pp. 301–313). Oxford University Press (OUP). https://doi.org/10.1093/gji/ggw033

Roth, D. L., Brodsky, E. E., Finnegan, N. J., Rickenmann, D., Turowski, J. M., & Badoux, A. (2016). Bed load sediment transport inferred from seismic signals near a river. *Journal of Geophysical Research: Earth Surface*, *121*(4), 725–747. https://doi.org/10.1002/2015jf003782

Schmandt, B., Aster, R. C., Scherler, D., Tsai, V. C., & Karlstrom, K. (2013). Multiple fluvial processes detected by riverside seismic and infrasound monitoring of a controlled flood in the Grand Canyon. In *Geophysical Research Letters* (Vol. 40, Issue 18, pp. 4858– 4863). American Geophysical Union (AGU). https://doi.org/10.1002/grl.50953

Schmandt, B., Gaeuman, D., Stewart, R., Hansen, S. M., Tsai, V. C., & Smith, J. (2017). Seismic array constraints on reach-scale bedload transport. In *Geology* (Vol. 45 Issue 4, pp. 299-304. https://doi.org/10.1130/g38639.1

Stark, K., Cadol, D., Laronne, J.B., Varyu, D., Halfi, E., Richards, M., 2019. "Initial Calibration of Acoustic Pipe Microphone Sensors to Monitor Bedload During Flash Floods in the Arroyo de los Piños, NM" SedHyd2019, Federal Interagency Sedimentation and Hydrologic Modeling Conference. June 2019, Reno NV.

Stark, K., Cadol, D., Varyu, D., & Laronne, J. B. (2021). Direct, continuous measurements of ultra-high sediment fluxes in a sandy gravel-bed ephemeral river. In *Geomorphology* (Vol. 382, p. 107682). Elsevier. https://doi.org/10.1016/j.geomorph.2021.107682

Tsai, V. C., Minchew, B., Lamb, M. P., & Ampuero, J.-P. (2012). A physical model for seismic noise generation from sediment transport in rivers. *Geophysical Research Letters* (Vol. 39, Issue 2, p. n/a-n/a). https://doi.org/10.1029/2011gl050255

Turowski, J. M., Badoux, A., & Rickenmann, D. (2011). Start and end of bedload transport in gravel-bed streams. *Geophysical Research Letters*, *38*(4). https://doi.org/10.1029/2010gl046558

US Department of Commerce, N. O. A. A. (2016, September 28). NWS ABQ High Wind Climatology. National Weather Service. Retrieved October 21, 2022, from https://www.weather.gov/abq/features_highwind

Welch, P. (1967). The use of fast fourier transform for the estimation of Power Spectra: A method based on time averaging over short, modified periodograms. *IEEE Transactions on Audio and Electroacoustics*, *15*(2), 70–73. https://doi.org/10.1109/tau.1967.1161901

Withers, M. M., Aster, R. C., Young, C. J., & Chael, E. P. (1996). High-frequency analysis of seismic background noise as a function of wind speed and shallow depth. *Bulletin of the Seismological Society of America*, *86*(5), 1507-1515.